

Robust and Fast Estimation of Signal-Dependent Noise in Medical X-Ray Image Sequences

Marc Hensel¹, Bernd Lundt², Thomas Pralow² and Rolf-Rainer Grigat¹

¹Vision Systems, TU Hamburg-Harburg, 21079 Hamburg

²General X-Ray, Philips Medical Systems, 22335 Hamburg

Email: marc.hensel@tu-harburg.de

Abstract. We present a practice-oriented, i.e. fast and robust, estimator for strong signal-dependent noise in medical low-dose X-ray images. Structure estimation by median filtering has shown to be superior to linear binomial filtering. Falsifications due to remaining structure in the estimated noise image are significantly reduced by iterative outlier removal.

1 Introduction

Medical X-ray image sequences as applied, e.g., in angiography exhibit severe signal-dependent noise. This is founded on low X-ray doses used for radiation protection reasons. Noise reduction as well as contrast enhancement methods can be significantly improved by consideration of the signal-dependent noise level. However, in noise estimation several intricacies arise.

First of all, the application requires real-time processing while sophisticated noise estimators exhibit high computing time (complexity). Also, there is the problem of structure diversity. Noise estimation implies signal estimation (object structures). However, clinical sequences contain large regions of low contrast and smooth transitions (e.g. organs) as well as fine structures of high contrast (e.g. catheters, vascular trees). Finally, existing noise models are not universally applicable for all observed X-ray images.

Existing noise models are based on the Poisson distribution as noise in low-dose X-ray images is dominated by statistical variability of the X-ray quanta and, thus, by additive Poisson-distributed quanta noise. However, all too often such distribution cannot be observed in medical sequences.

Flat-panel detectors might consist of multiple detector arrays exhibiting significantly differing properties (e.g. sensitivity) and, hence, require corrective preprocessing. Moreover, device-specific logarithmic mappings of digital X-ray images with the purpose to establish linear dependency of gray-values from the thickness of imaged objects are applied. These mappings invert the monotony of signal-dependent noise curves. Even worse, mapping parameters not matching the detector or camera type can totally degrade the noise curve. As concluding example, preprocessing by Wiener filtering leads to a sharp bend in noise curves that cannot be described by the known models.

2 State-of-the-Art

State-of-the-art noise models for low-dose X-ray images are based on the assumption of the data being dominated by additive Poisson-distributed quanta noise. In Poisson-distributed data, mean μ (i.e. the expected uncorrupted signal intensity $s(x, y)$) equals variance σ^2 . Thus, noise standard deviation $\sigma = \sqrt{\mu}$ increases with the square root of the expected signal strength. Most often, and leading to a differing model, the exponential attenuation of X-rays passing through matter is compensated by logarithmic mapping. Hereby, linear dependency of image intensity and traversed object thickness is established. At the same time, logarithmic mapping fundamentally changes the noise characteristic. The resulting noise standard deviation is monotonically decreasing over large signal ranges and can be modeled by an exponential function. However, both models are device-specific and preprocessing might yield observed noise characteristics that are not adequately described by these models.

There are a multitude of noise estimation methods [1]. Many of these are not suited for real-time X-ray image processing, because of the huge amount of data, the complexity of the method, or because they are not suited for signal-dependent noise. Examples are methods based on wavelet transformation or Maximum Likelihood estimation [2, 3]. Noise estimators for real-time applications are mostly based on signal estimation by low-pass filtering. The high-pass portion, i.e. the data filtered out, is interpreted as noise and analyzed to yield the noise estimation [1, 4]. Naturally, the resulting noise estimation can be considerably falsified by structure, as edges contain significant high-frequency components.

3 Methods

In the context of real-time noise estimation, three major questions arise: What are the noise properties? Which filter is suited to approximate the signal? Finally, how can the influence of signal on the estimated noise image be further reduced?

3.1 Noise Model

The physical process underlying noise in low-dose X-ray images is Poisson-distributed quanta noise. For a – in practice fulfilled – ”sufficiently large” number of quanta contributing per pixel (about 20), the discrete distribution can be approximated by the continuous normal (Gaussian) distribution with same mean and variance. Our measurements of X-rayed brass wedges using varying preprocessing steps verified that the observed signal-dependent noise can be described fairly well by additive zero-mean normal-distributed noise η with signal-dependent standard deviation $\sigma_\eta(s)$, i.e.

$$g(x, y) = s(x, y) + \eta(s(x, y)) \quad (1)$$

$$\text{pdf}(\eta; s) = \frac{1}{\sqrt{2\pi} \cdot \sigma_\eta(s)} \exp\left(-\frac{1}{2} \left(\frac{\eta}{\sigma_\eta(s)}\right)^2\right) \quad (2)$$

with signal s and the observed gray-valued image g .

Table 1. Noise estimation in homogeneous images using 3×3 standard filters

Filter	σ_{s_e}/σ_0	σ_{η_e}/σ_0	ϵ_{η_e} [%]
Median	0.4078	0.9720	2.85
Binomial	0.3750	0.8004	19.96

3.2 Signal Estimation Filter

With estimated signal s_e , the estimated noise component at location (x, y) is given by $\eta_e(x, y) = g(x, y) - s_e(x, y)$. For real-time signal estimation in very noisy images, 3×3 median and (linear) binomial filters h are taken into account [1]. In homogeneous signals $s(x, y) = s_0$ corrupted by noise σ_0 , linear filtering $s_e = h * g$ yields an estimated noise image η_e with standard deviation $\sigma_{\eta_e}^2$ according to:

$$\sigma_{\eta_e}^2 = \left[\sum_i \sum_j [1 - \delta(i)\delta(j)] h_{i,j}^2 + (1 - h_{0,0})^2 \right] \cdot \sigma_0^2 \quad (3)$$

The performance of median filtering has been analyzed by experiments.

For both, median and binomial filtering, Table 1 shows the noise levels in s_e and η_e as well as the relative error $\epsilon_{\eta_e} = |\sigma_{\eta_e} - \sigma_0|/\sigma_0$ of the resulting noise estimation. Regarding s_e , noise reduction performance of the median filter is only slightly below the binomial filter. However, most remarkably, noise in η_e reflects σ_0 by far better than in case of the binomial filter. Furthermore, median filtering is superior in structure preservation and, thus, in limiting the influence of signal structure on η_e .

3.3 Intra-Frame Noise Estimation

The proposed method is organized in five steps:

1. Signal estimation $s_e(x, y)$ by 3×3 median filtering and creation of the corresponding noise image $\eta_e(x, y) = g(x, y) - s_e(x, y)$
2. Subdivision of the dynamic range of the signal in intervals S_i of equal size
3. Estimation of noise $\sigma_{\eta_e}(i)$ in the intervals $S(i)$ as standard deviation of all noise values $\eta_e(x, y)$ whose corresponding signal values $s_e(x, y)$ are in S_i
4. Iterative outlier removal
5. Interpolation with consideration of the statistical basis

The quality of the initial noise estimation in $S(i)$

$$\sigma_{\eta_e}(i) = E \left\{ (N_i - E\{N_i\})^2 \right\}^{-1/2} \quad \text{with} \quad (4)$$

$$N_i = \left\{ \eta_e(x, y) \mid s_e(x, y) \in S_i \right\} \quad (5)$$

is improved by iterative outlier removal: In the calculation of the noise standard deviation $\sigma_{\eta_e}(i)$ for an interval $S(i)$, absolute noise values above three times the

standard deviation are with high probability caused by high-frequency components originating from structure and not from noise. Thus, these outliers are removed from $N_i(t)$ iteratively and the standard deviation is updated from the remaining values in $N_i(t+1)$:

$$N_i(t+1) = \left\{ \eta_e(x, y) \mid \eta_e(x, y) \in N_i(t) \wedge |\eta_e(x, y)| \leq 3\sigma_{\eta_e}(i) \right\} \quad (6)$$

The noise estimations $\sigma_{\eta_e}(i)$ for intervals S_i are mapped to a signal-dependent estimation $\sigma_{\eta_e}(s)$ by interpolation of $\sigma_{\eta_e}(i)$ of those intervals, where a "sufficiently high" number (> 100) of pixel values have contributed to the standard deviation. Clinical X-ray images most often contain smooth transitions. Hence, normally most intervals are considered in the interpolation for the number of intervals (e.g. 128) and image data used by our groups.

3.4 Incremental Inter-Frame Noise Estimation

For applications with very restrictive real-time requirements, the computing time for noise estimation can be controlled adaptively by incremental inter-frame noise estimation. Founded on the expression $\sigma^2(X) = E(X^2) - E(X)^2$, the basic idea is to incrementally improve the estimation by additional consideration of some pixels of each new frame in a sequence. Number and location of the pixels is arbitrary, however, locations should differ from image to image in such way that all image coordinates have the same contribution in the long run. Incremental adding can be applied as long as the imaging parameters are constant and, hence, frames exhibit equivalent noise characteristics.

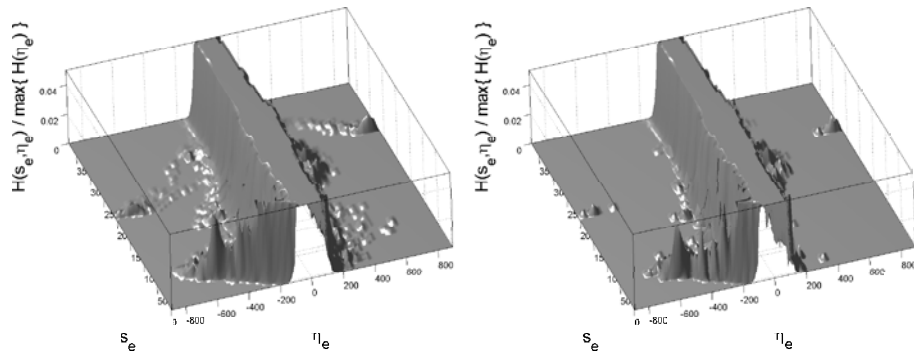
4 Results

Signal-dependent noise in low-dose X-ray images is described well by additive zero-mean Gaussian noise with signal-dependent standard deviation. The maximum absolute difference of normal and Poisson distributions of equal mean and variance is solely 0.010 units (normed to signal values: 0.10%) for 10 quanta per pixel and 0.005 units (0.02%) for 20 quanta per pixel. The measured noise curves $\sigma_{\eta_e}(s)$ are quasi-continuous, but not necessarily monotonic.

The precision of the noise estimation has been evaluated using uniform, artificial, and clinical test images corrupted by noise with known characteristic. The clinical image showing a vascular tree has been acquired with comparatively high dose and, thus, contains low noise. This was further reduced by nonlinear diffusion filtering prior to evaluation.

On all test data, signal estimation by median filtering clearly outperformed estimation based on binomial filtering. In the absence of image structure, the relative error of the estimated noise was about 2.85% for median and 19.96% for binomial filtering (Tab. 1). The presence of artificial structure falsified the noise estimation and yielded relative errors of 52.18% (median) and 81.69% (binomial). In the presented method, these errors were significantly reduced, in

Fig. 1. Estimated noise histograms for binomial filtering of clinical image. IDEAL CASE: 1-D histograms for constant s_e are Gaussian-distributed. LEFT: All pixels contribute. Structure produces errors with predominantly negative/positive sign for small/large s_e (MSE: 8.96). RIGHT: Only 37.16% of pixels with lowest entries ($\leq 1\%$ max. value) in edge image (Prewitt) contribute. Strong disturbances due to structure remain (MSE: 7.54). PROPOSED METHOD: The disturbances are largely removed (MSE: 3.34). (For better visibility the data is normed to 1 for each s_e and the display clipped to 0.05.)



particular by structure iteration, to about 0.05% (median) and 17.38% (binomial), respectively. For the clinical image, relative estimation errors were about 2.67% and 18.91%, respectively. State-of-the-art gradient-based methods [1] did not yield comparable reduction of the influence of structure for the clinical test image (see Figure 1 and mean squared errors of normed data therein).

5 Discussion

The presented method is utmost robust in several aspects. Most prominent are its universality and suppression of object structures. The method adapts to the noise characteristics and is suited for exposures and fluoroscopic sequences, likewise. Moreover, typical falsifications in state-of-the-art noise estimators due to high-frequency components of structure are significantly reduced by iterative outlier removal. Finally, it has shown that signal estimation using median filtering yields good results for images corrupted by severe noise (e.g. fluoroscopic images).

References

1. Olsen SI. Estimation of noise in images: An evaluation. *CVGIP: Graphical Models and Image Processing* 1993;55(4):319–323.
2. Yuan X, Buckles BP. Subband Noise Estimation for Adaptive Wavelet Shrinkage. In: *Proc IEEE 17th Int Conf Pattern Recognition*. vol. 4; 2004. p. 885–888.
3. Sijbers J, den Dekker AJ. Maximum Likelihood Estimation of Signal Amplitude and Noise Variance From MR Data. *Magn Reson Med* 2004;51(3):586–594.
4. Amer A, Dubois E. Fast and Reliable Structure-Oriented Video Noise Estimation. *IEEE Trans Circuits and Systems for Video Technology* 2005;15(1):113–118.